Two tetrodotoxin-resistant sodium channels in human dorsal root ganglion neurons

S.D. Dib-Hajj[a,b,c], L. Tyrrell[a,b,c], T.R. Cummins[a,b,c], J.A. Black[a,b,c], P.M. Wood[d], S.G. Waxman[a,b,c,*]

[a] *Department of Neurology LCI 707, Yale University School of Medicine, 333 Cedar Street, New Haven, CT 06510, USA*
[b] *PVA/EPVA Neuroscience Research Center, Yale University School of Medicine, 333 Cedar Street New Haven, CT 06510, USA*
[c] *Rehabilitation Research Center, Veterans Affairs Medical Center, West Haven, CT 06516, USA*
[d] *Miami Project to Cure Paralysis and Department of Neurological Surgery, University of Miami School of Medicine, Miami, FL 33136, USA*

Received 4 October 1999

Abstract Two tetrodotoxin-resistant (TTX-R) voltage-gated sodium channels, SNS and NaN, are preferentially expressed in small dorsal root ganglia (DRG) and trigeminal ganglia neurons, most of which are nociceptive, of rat and mouse. We report here the sequence of NaN from human DRG, and demonstrate the presence of two TTX-R currents in human DRG neurons. One current has physiological properties similar to those reported for SNS, while the other displays hyperpolarized voltage-dependence and persistent kinetics; a similar TTX-R current was recently identified in DRG neurons of sns-null mouse. Thus SNS and NaN channels appear to produce different currents in human DRG neurons.

Key words: Na current kinetics; Spinal sensory neuron; Nociceptive neuron

1. Introduction

Voltage-gated sodium channels play critical roles in electrogenesis in most excitable cells, including dorsal root ganglion (DRG) neurons. DRG neurons are unusual in expressing prominent sodium currents that are resistant to tetrodotoxin (TTX-R) [1–4]. TTX-R currents are increased in experimental models of inflammatory pain or when DRG cultures are exposed to inflammatory modulators such as the prostaglandin PGE_2 [5–8]. Furthermore, TTX-R currents appear to participate in the transmission of nociceptive signals from the periphery to the central nervous system as they are important for conduction in C-fibers and the release of the neurotransmitter CGRP from nociceptors and the stimulation of spinal cord dorsal horn neurons via C-fiber activation [9–11]. One TTX-R sodium channel, termed SNS [12] and PN3 [13], was initially cloned from the rat, with subsequent cloning of its mouse and human cognates [14,15]. A second TTX-R sodium channel, initially termed NaN [16] and subsequently termed SNS2 [17], has been cloned from the rat and the mouse DRG [18]. Here we report the sequence of the human cognate of NaN, and show the presence of two distinct TTX-R sodium currents, one with properties that correspond to those reported for SNS, and the other with novel properties, in human DRG neurons.

*Corresponding author. Fax: (1) (203) 785-7826.
E-mail: stephen.waxman@yale.edu

2. Materials and methods

2.1. Isolation of human NaN

Human DRGs were obtained from organ donors with full legal consent for use of tissue for research. Total RNA extraction and cDNA synthesis were performed as described previously [16]. Extraction buffer was used at 25 μl per 1 mg of tissue. For initial discovery and analytical applications, first strand cDNA was reverse transcribed in a 25 μl final volume using total RNA, 1 mM random hexamer (Boehringer Mannheim), 500 units SuperScript II reverse transcriptase (Life Technologies) and 100 units of RNase Inhibitor (Boehringer Mannheim). The buffer consisted of 50 mM Tris-HCl (pH 8.3), 75 mM KCl, 3 mM $MgCl_2$, 10 mM DTT and 5 mM dNTP. The reaction was allowed to proceed at 37°C for 90 min, 42°C for 30 min, then terminated by heating to 65°C for 10 min. For 5′ and 3′ RACE, marathon cDNA was constructed as previously described [16]. PCR amplification was performed in 60 μl volume using 1 μl of first strand cDNA, 0.8 μM of each primer and 1.75 units of Expand Long Template DNA polymerase enzyme mixture (Boehringer Mannheim). Amplification was carried out using a programmable thermal cycler (PTC-100, MJ Research, Cambridge, MA, USA) via: (1) initial denaturation at 92°C for 2 min; (2) 35 cycles of denaturation at 92°C for 20 s, annealing at 60°C for 1 min and elongation at 72°C for 2 min; (3) elongation at 72°C for 10 min. Sequencing was carried out at the HHMI/Keck Biotechnology Resource Laboratory at Yale University. Sequence analysis was performed using BLAST (National Library of Medicine), Genetics Computer Group (Madison, WI, USA) and Lasergene (DNASTAR, Madison, WI, USA) software. The human NaN sequence has been deposited with the EMBL/GenBank data libraries under the accession number AF188679.

2.2. Cell culture

The DRGs were harvested within 2 h of clamping the aorta and dissociated within 24 h of clamping. Nerve roots and as much connective tissue as possible were removed and 2 or 3 DRGs were sliced into small fragments in enzyme solution containing 0.2% collagenase (Worthington, Type 1) and 0.5% dispase II (Boehringer-Mannheim) in Ca^{2+}/Mg^{2+}-free Hanks' balanced salt solution. The fragment-enzyme solution was incubated on a rotating shaker at 37°C for 1 h. The tissue fragments were collected by centrifugation, rinsed twice in L-15 medium (Gibco) with 10% heat-inactivated fetal bovine serum and then triturated using a pipet with a reduced tip to produce a crude cell suspension. The cell suspension was rinsed twice in Ca^{2+}/Mg^{2+}-free Hanks' solution with 15% Percoll to remove myelin debris. The final cell pellet was resuspended in Dulbecco's modified Eagle/Ham F-12 medium without additives. Cells were plated onto collagen-coated 12 mm circular glass coverslips, allowed to adhere for 1 h, then flooded with Dulbecco's modified Eagle/Ham F-12 with 10% fetal bovine serum and maintained in a humidified 5% CO_2/air atmosphere at 37°C. Small DRG neurons were examined by whole-cell patch clamp <24 h following plating.

2.3. Whole-cell recordings

Whole-cell patch clamp recordings were conducted at room temperature (21°C) using an EPC-9 amplifier. Data were acquired on a Macintosh Quadra 950 using the Pulse program (v 7.89, HEKA Electronic, Germany). Fire-polished electrodes (0.8–1.5 MW) were fabricated from 1.65 mm capillary glass (Drummond) using a Sutter P-87

0014-5793/99/$20.00
PII: S0014-5793(99)01519-7

puller. To optimize space clamp, only isolated cells with a soma size of <30 μm were used. Voltage errors were minimized using 80% series resistance compensation and the capacitance artifact was canceled using the amplifier computer-controlled circuitry. Linear leak subtraction was used for all voltage clamp recordings. Membrane currents were filtered at 5 kHz and sampled at 20 kHz. The pipette solution contained: 140 mM CsF, 1 mM EGTA and 10 mM Na-HEPES (pH 7.3). The standard bathing solution was 140 mM NaCl, 3 mM KCl, 1 mM $MgCl_2$, 1 mM $CaCl_2$ and 10 mM HEPES (pH 7.3). Data were not corrected for liquid junction potentials, which were <5 mV. The osmolarity of all solutions was adjusted to 310 mOsm.

3. Results

A fragment of human NaN (hNaN) was obtained using our original multiplex PCR approach, which identified rat and mouse NaN [16,18]. This approach produced a 474 bp fragment from domain I encoding part of S3 to the N-terminal part of the extracellular loop between S5 and S6. Additionally, we identified and used two pairs of published human EST sequences (AA446997/AA446878 and AA885211/AA913881) which show the highest homology to NaN sequences from rat (rNaN) and mouse (mNaN); all four ESTs show partial intron sequences at positions where introns are present in Scn11a, the gene encoding mNaN [18]. The predicted amino acid sequence of the coding portion of the 5′ most EST starts in the S4 segment of domain II (DII-S4), while the coding sequence of the 3′ most EST ends in the linker joining segments S3 and S4 of domain IV. Using hNaN-specific primers complementary to the fragment in domain 1 and the 3′ most EST, the hNaN sequence was extended from S3 in domain 1 to S4 in domain 4. Sequences extending to the translation initiation ATG and to the 3′ untranslated sequence of this gene were determined from fragments produced by 5′ and 3′ RACE, respectively, similar to the manner in which rNaN and mNaN sequences were determined [16,18]. Human NaN cDNA encodes a polypeptide sequence of 1792 amino acids (Fig. 1), which is slightly longer than rNaN and mNaN at 1765 amino acids [16,18]. Human NaN amino acid sequence is 80% similar (74.6% identical) to both rNaN and mNaN, while mNaN is 91% similar (89% identical) to rNaN. The sequence identity of NaN among the three species is lower than that reported for other α-subunits [14,19]. Compared to rat and mouse NaN, most of the divergent amino acids, including insertions, are clustered in extracellular linkers in domains I, II and III, in the cytoplasmic loop connecting domains II and III, and the C-terminal region. Not surprisingly, mNaN shows most of the changes compared to rNaN at these locations. It is possible that these regions tolerate change more than other parts of the channel; however, the clustering of these changes may also have a functional significance. The extracellular linkers are expected to contribute to the structure of the extracellular mouth of the channel and various neurotoxins are known to bind in these regions [20–24]. These changes may be caused by adaptive co-evolution of sequences in the different species to maintain tertiary interactions within the channels or to accommodate interaction with species-specific extracellular and intracellular proteins [18].

The TTX phenotype determinant amino acid in DI-SS2, serine (S^{360}), indicates that hNaN is a TTX-R channel. The inactivation tripeptide IFM [25] is conserved within L3 of human NaN as is the consensus PKC phosphorylation site, serine (S^{1341}). Like rNaN and mNaN, hNaN contains multiple predicted phosphorylation sites in the L1 and L2 loops. Surprisingly, and unlike rNaN and mNaN, the S4 segment of hNaN has the same number of positively charged residues as other members of subfamily 1. The first predicted charged residue, arginine (R^{670}) in DII-S4, is replaced by an alanine residue in both rNaN (A^{664}) and mNaN (A^{666}). This change may cause a shift in the voltage-dependence of hNaN compared to rNaN and mNaN. However, like rNaN and mNaN, hNaN has one less positively charged residue at the C-terminal end of DIII-S4, compared to SNS, rH1 and the other members of subfamily 1. The number of the positively charged residues in the DI-S4 and DIV-S4 segments are identical to those in subfamily 1. We examined the TTX-R sodium currents in human small DRG neurons (diameter <30 μm) using whole-cell patch clamp recordings. We were able to obtain recordings from a limited number of small DRG neurons, with 12–14 neurons displaying large TTX-R currents. Slowly inactivating and persistent TTX-R sodium currents

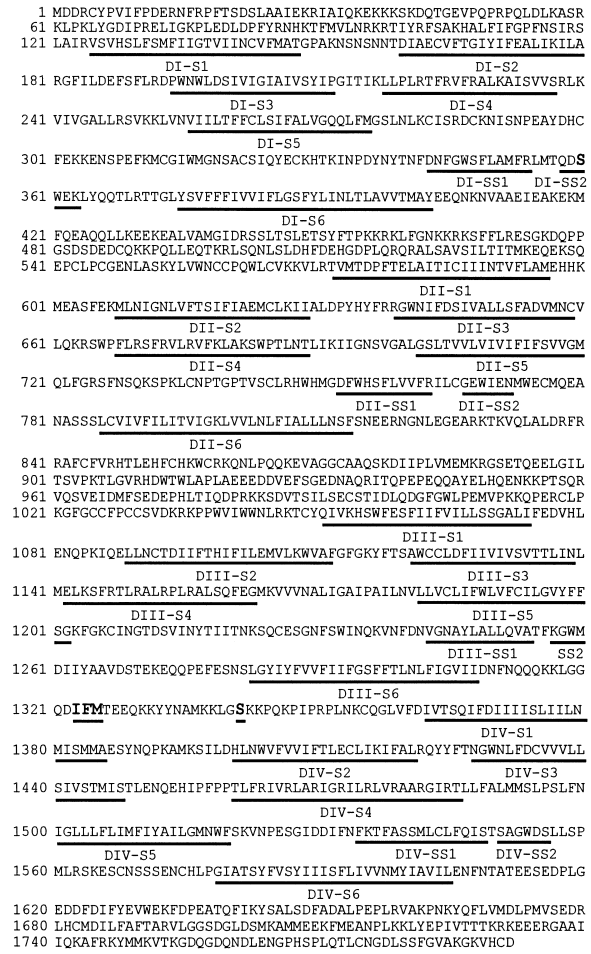

Fig. 1. Predicted amino acid sequence of human NaN. DI-DIV represent the four domains of Na channels with the putative transmembrane segments underlined. The serine residue of DI-SS2 predicted to underlie the TTX-R phenotype (S^{360}), the PKC phosphorylation site in L3 (S^{1341}), and the tripeptide IFM in L3 involved in fast inactivation, are in bold, larger type and underlined. A sequence of 6237 bp contains the 5376 ORF, 30 bp of 5′UTR, and 832 bp 3′UTR. The 3′UTR contains 273 bp with high similarity to AluI-Sc subfamily consensus sequence (GenBank accession number U14571).

could be elicited with depolarizing steps from a holding potential of −120 mV (Fig. 2A). The slowly inactivating current predominates when the cells are depolarized from a holding potential of −60 mV (Fig. 2B). The persistent TTX-R current can be obtained by digitally subtracting the current obtained with $V_{hold} = -60$ mV from that obtained with $V_{hold} = -120$ mV (Fig. 2C). Using gene knock-out technology, SNS was recently shown to encode the slowly inactivating component of the TTX-R sodium current [26]. We have recently shown that in these sns-null mutant mice, small diameter DRG neurons express the persistent TTX-R sodium current in the absence of slowly inactivating TTX-R current; we also found that the slowly inactivating current and the persistent current in wild-type mouse DRG neurons can be separated by varying the holding potential (Cummins et al., unpublished). These two distinct TTX-R currents thus appear to be generated by different genes in mice DRG neurons. Seven of the 14 human DRG neurons displayed a mixture of the slowly inactivating and persistent TTX-R sodium currents. Of the remaining neurons that had TTX-R sodium currents, three displayed predominantly slowly inactivating SNS-type currents (Fig. 3A) and two displayed predominantly persistent TTX-R sodium currents (Fig. 3B). The voltage-dependence of activation (Fig. 3C) and inactivation (Fig. 3D) for the human slowly inactivating SNS-type TTX-R sodium current is similar to that previously reported in rat, mice and human DRG neurons [27–29]. The persistent TTX-R current is similar to the persistent TTX-R sodium current that we have identified in sns-null and wild-type mouse small DRG neurons (Cummins et al., unpublished). However, the voltage-dependence of activation appears more hyperpolarized for the human persistent TTX-R sodium current (Fig. 3C) than for the mouse persistent TTX-R sodium current (threshold ∼−65 mV, $V_{1/2} \sim -45$ mV). Because of the overlap between activation and steady-state inactivation, step depolarizations to voltages near typical resting potential can elicit TTX-R sodium currents in human DRG neurons that persist for more than 2 s (Fig. 3E). Although this persistent current can display an amplitude >10 nA if elicited from negative holding potentials, it is significantly reduced by holding the cells at more depolarized potentials due to ultra-slow inactivation. Recovery of the human persistent TTX-R sodium current is slow, with a time constant of ∼60 s at −120 mV, which is similar to that observed for the mouse persistent TTX-R current.

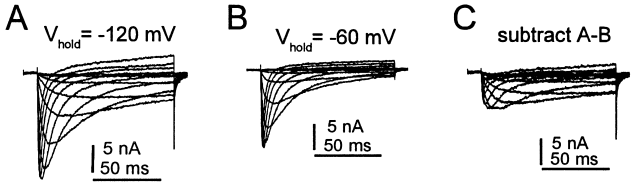

Fig. 2. Multiple TTX-R sodium currents are expressed in human small DRG neurons. A: Representative recordings from a holding potential of −120 mV. Calcium currents were blocked with 100 μM cadmium in the bath solution and TTX (250 nM) blocked the fast-inactivating currents. B: When the same neuron was held at −60 mV and a 500 ms step to −120 mV preceded the test pulses, the persistent current was attenuated. C: Subtraction of the slowly inactivating component (B) from the total TTX-R current (A) reveals the persistent current in the human DRG neuron.

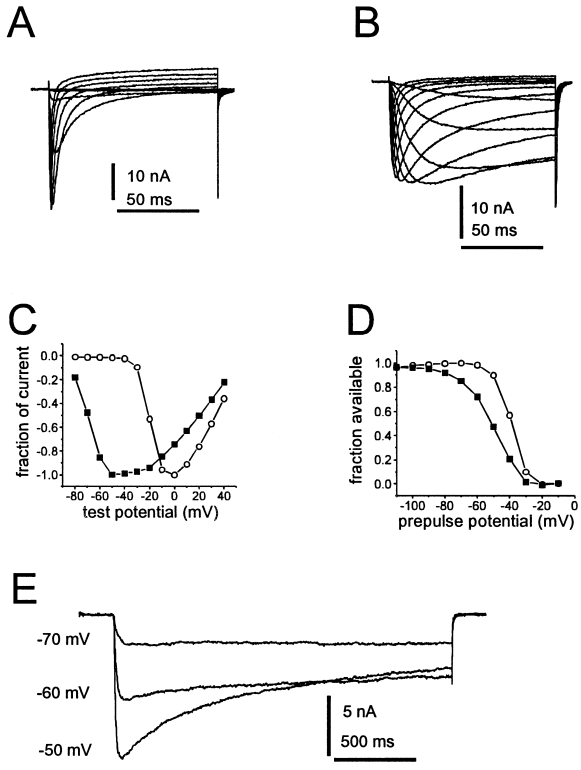

Fig. 3. A: Example of a human DRG neuron that displayed primarily slowly inactivating TTX-R currents (holding potential = −120 mV). B: Example of a human neuron that displayed primarily persistent TTX-R currents (holding potential = −120 mV). C: The current-voltage relationship is shown for the cells in (A) (unfilled circles) and (B) (filled squares). Note that the persistent TTX-R current exhibits substantial activation at −80 mV, but the slowly inactivating current does not activate until about −30 mV. D: Steady-state inactivation curves are shown for the TTX-R current in the cells shown in (A) (unfilled circles) and (B) (filled squares). Steady-state inactivation was measured with 500 ms prepulses. $V_{test} = -10$ mV. E: TTX-R persistent currents from a human small DRG neuron elicited with 2 s step depolarizations to the voltage indicated. Note that at −70 mV there is very little inactivation of this current during the 2 s depolarization.

4. Discussion

We report the sequence of a second TTX-R sodium channel (hNaN) which is present, together with SNS, in human DRG neurons. We also report the presence, in these cells, of two distinct TTX-R sodium currents including a novel, persistent TTX-R current that is likely to arise from the NaN channel. SCN11A, the human gene encoding NaN, was recently mapped to chromosome 3, in close proximity to SCN5A and SCN10A, the genes encoding the two other TTX-R sodium channels, SkM2 and SNS, respectively [18]. The three genes thus appear to share a common lineage. The fact that PCR amplification of human, rat and mouse NaN produces only one sequence strongly suggests that there is only one copy of this gene on this chromosome. Our data also demonstrate the presence, in human DRG neurons, of two distinct sodium currents, one with properties that correspond to those reported previously for SNS [12,13,26]. The second TTX-resistant sodium current has a number of novel properties, including a hyperpolarized voltage-dependence of steady-state inactivation. This current is also notable in displaying a rela-

tively hyperpolarized voltage-dependence for activation, and persistent kinetics. The persistent TTX-R current in human DRG neurons appears to activate around −80 mV. This is 10–20 mV more negative than the persistent TTX-R sodium current in sns-null and wild-type mouse DRG neurons. Although the data set is limited, this is an intriguing observation, because mNaN and rNaN have one fewer charge in DII-S4 segment compared to the hNaN. Several studies have shown that neutralization of the analogous R in the skeletal muscle and cardiac sodium channel isoforms shifts the voltage-dependence of activation in the depolarizing direction [30–33], consistent with the apparent difference in the activation of human and mice persistent TTX-R currents.

We have previously recorded a similar persistent TTX-resistant sodium current (Cummins et al., unpublished) in sns-null mice that do not express the SNS α-subunit [26]. Since the presence of only two TTX-resistant sodium channels (SNS and NaN) has been demonstrated in DRG neurons, and since the slowly inactivating TTX-resistant sodium current that we observed in human DRG neurons has physiological properties similar to those previously reported for SNS, it appears likely that the novel, persistent sodium current that we have observed in human DRG neurons is produced by NaN channels. In summary, our results demonstrate the presence of two distinct TTX-R sodium channels in human DRG neurons and suggest that they play different functional roles in these cells.

Acknowledgements: Adult human DRG was kindly provided by Les Olson and the University of Miami Organ Procurement Team. This work was supported in part by grants from the Medical Research Service and the Rehabilitation Research Service, Department of Veterans Affairs, and by grants from The Eastern Paralyzed Veterans Association and the Paralyzed Veterans of America (S.G.W.), and NINDS Grant NS09923-28 (P.W.).

References

[1] Kostyuk, P.G., Veselovsky, N.S. and Tsyndrenko, A.Y. (1981) Neuroscience 6, 2423–2430.
[2] Roy, M.L. and Narahashi, T. (1992) J. Neurosci. 12, 2104–2111.
[3] Caffrey, J.M., Eng, D.L., Black, J.A., Waxman, S.G. and Kocsis, J.D. (1992) Brain Res. 592, 283–297.
[4] Elliott, A.A. and Elliott, J.R. (1993) J. Physiol. 463, 39–56.
[5] England, S., Bevan, S. and Docherty, R.J. (1996) J. Physiol. 495, 429–440.
[6] Gold, M.S., Reichling, D.B., Shuster, M.J. and Levine, J.D. (1996) Proc. Natl. Acad. Sci. USA 93, 1108–1112.
[7] Tanaka, M., Cummins, T.R., Ishikawa, K., Dib-Hajj, S.D., Black, J.A. and Waxman, S.G. (1998) NeuroReport 9, 967–972.
[8] Khasar, S.G., Gold, M.S. and Levine, J.D. (1998) Neurosci. Lett. 256, 17–20.
[9] Jeftinija, S. (1994) Brain Res. 665, 69–76.
[10] Jeftinija, S. (1994) Brain Res. 639, 125–134.
[11] Brock, J.A., McLachlan, E.M. and Belmonte, C. (1998) J. Physiol. 512, 211–217.
[12] Akopian, A.N., Sivilotti, L. and Wood, J.N. (1996) Nature 379, 257–262.
[13] Sangameswaran, L. et al. (1996) J. Biol. Chem. 271, 5953–5956.
[14] Souslova, V.A., Fox, M., Wood, J.N. and Akopian, A.N. (1997) Genomics 41, 201–209.
[15] Rabert, D.K. et al. (1998) Pain 78, 107–114.
[16] Dib-Hajj, S.D., Tyrrell, L., Black, J.A. and Waxman, S.G. (1998) Proc. Natl. Acad. Sci. USA 95, 8963–8968.
[17] Tate, S. et al. (1998) Nat. Neurosci. 1, 653–655.
[18] Dib-Hajj, S.D., Tyrrell, L., Escayg, A., Wood, P.M., Meisler, M.H. and Waxman, S.G. (1999) Genomics 59, 309–318.
[19] Plummer, N.W., Galt, J., Jones, J.M., Burgess, D.L., Sprunger, L.K., Kohrman, D.C. and Meisler, M.H. (1998) Genomics 54, 287–296.
[20] Rogers, J.C., Qu, Y., Tanada, T.N., Scheuer, T. and Catterall, W.A. (1996) J. Biol. Chem. 271, 15950–15962.
[21] Penzotti, J.L., Fozzard, H.A., Lipkind, G.M. and Dudley, S.C. (1998) Biophys. J. 75, 2647–2657.
[22] Li, R.A., Tsushima, R.G., Kallen, R.G. and Backx, P.H. (1997) Biophys. J. 73, 1874–1884.
[23] Chahine, M., Sirois, J., Marcotte, P., Chen, L. and Kallen, R.G. (1998) Biophys. J. 75, 236–246.
[24] Cestele, S. et al. (1999) Eur. J. Neurosci. 11, 975–985.
[25] West, J.W., Patton, D.E., Scheuer, T., Wang, Y., Goldin, A.L. and Catterall, W.A. (1992) Proc. Natl. Acad. Sci. USA 89, 10910–10914.
[26] Akopian, A.N. et al. (1999) Nat. Neurosci. 2, 541–548.
[27] McLean, M.J., Bennett, P.B. and Thomas, R.M. (1988) Mol. Cell. Biochem. 80, 95–107.
[28] Rush, A.M., Brau, M.E., Elliott, A.A. and Elliott, J.R. (1998) J. Physiol. 511, 771–789.
[29] Cummins, T.R. and Waxman, S.G. (1997) J. Neurosci. 17, 3503–3514.
[30] Chen, L.Q., Santarelli, V., Horn, R. and Kallen, R.G. (1996) J. Gen. Physiol. 108, 549–556.
[31] Kontis, K.J., Rounaghi, A. and Goldin, A.L. (1997) J. Gen. Physiol. 110, 763.
[32] Groome, J.R., Fujimoto, E., George, A.L. and Ruben, P.C. (1999) J. Physiol. 516, 687–698.
[33] Mitrovic, N., George, A.L. and Horn, R. (1998) J. Gen. Physiol. 111, 451–462.